

Polymer-like Conformation and Growth Kinetics of Bi_2S_3 Nanowires

Ludovico Cademartiri,^{†,‡,†} Gerald Guerin,[†] Kyle J. M. Bishop,[§] Mitchell A. Winnik,^{*,†} and Geoffrey A. Ozin^{*,†}

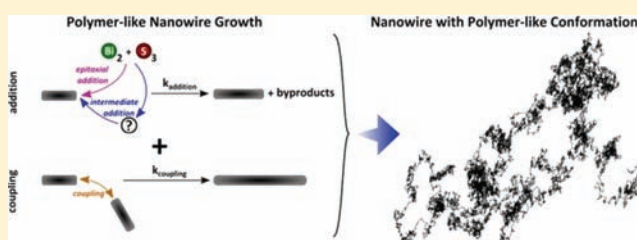
[†]Department of Chemistry, University of Toronto, 80 St. George Street, Toronto, Ontario M5S 1H6, Canada

[‡]Department of Chemistry and Chemical Biology, Harvard University, 12 Oxford Street, Cambridge, Massachusetts 02138, United States

[§]Department of Chemical Engineering, The Pennsylvania State University, University Park, Pennsylvania 16802, United States

Supporting Information

ABSTRACT: One-dimensional inorganic crystals (i.e., crystalline nanowires) are one of the most intensely investigated classes of materials of the past two decades. Despite this intense effort, an important question has yet to be answered: do nanowires display some of the unique characteristics of polymers as their diameter is progressively decreased? This work addresses this question with three remarkable findings on the growth and form of ultrathin Bi_2S_3 nanowires. (i) Their crystallization in solution is quantitatively describable as a form of living step-growth polymerization: an apparently exclusive combination of addition of “monomer” to the ends of the nanowires and coupling of fully formed nanowires “end-to-end”, with negligible termination and initiation. (ii) The rate constants of these two main processes are comparable to those of analogous processes found in polymerization. (iii) The conformation of these nanowires is quantitatively described as a worm-like conformation analytically analogous to that of semiflexible polymers and characterized by a persistence length of 17.5 nm (shorter than that of double-stranded DNA) and contour lengths of hundreds of micrometers (longer than those of most synthetic polymers). These findings do not prove a chemical analogy between crystals and polymers (it is unclear if the monomer is a molecular entity *tout court*) but demonstrate a physical analogy between crystallization and polymerization. Specifically, they (i) show that the crystallization of ensembles of nanoscale inorganic crystals can be conceptually analogous to polymerization and can be described quantitatively with the same experimental and mathematical tools, (ii) demonstrate that one-dimensional nanocrystals can display topological characteristics of polymers (e.g., worm-like conformation in solution), (iii) establish a unique experimental model system for the investigation of polymer-like topological properties in inorganic crystals, and (iv) provide new heuristic guidelines for the synthesis of polymer-like nanowires.



INTRODUCTION

Inorganic crystals display a range of physical properties (e.g., electrical,¹ optical,² magnetic,³ phase-change,⁴ ferroelectric,⁵ piezoelectric⁶) that are either uncommon or absent in organic crystals or polymers. In many cases, these physical properties depend strongly on the size and morphology of the crystal.^{7,8} Nanowires show weaker size effects on their physical properties than comparably sized spherical nanocrystals, due to the loss of confinement along one dimension. Therefore, the synthesis of particularly thin (<10 nm) nanowires is an intensely pursued and, until recently, curiously elusive objective.⁹

As new methodologies enable the synthesis of ever thinner nanowires, the cross-sectional dimensions and aspect ratios of these structures are approaching those of linear polymer molecules.^{10–12} This newfound similarity of sizes across the often ill-defined boundary between crystals and molecules can now be used to answer difficult and fascinating questions: Are crystallization and polymerization—the two processes by which we create most synthetic materials—blurring into each other at the nanoscale, as recent results on block copolymer micelles

suggest?¹³ Will the unique properties of polymers emerge in inorganic crystals when these are made one-dimensional and of near-molecular dimensions?

Polymer molecules possess topological properties (e.g., coil-like conformation in solution, viscoelasticity, thixotropy, reptation)¹⁴ that are central to their technological applications (e.g., glues, paints, rubbers, textiles) and are not found in other materials. A new class of materials that would intrinsically combine these properties with the physical properties of inorganic nanowires could be useful in a vast range of applications and provide new capabilities. The topological properties of polymers are a necessary consequence of their flexibility (i.e., dynamic fluctuation of the conformation in most thermal regimes used in practice) and of the typically large (up to $\sim 10^4$) ratio between the length of their backbone (L_n , the contour length), and their persistence length (p , which measures the persistence of orientational correlations along

Received: February 24, 2012

Published: April 25, 2012

the backbone).¹⁴ An object with $L_n/p \approx 1$ behaves like a rigid rod; an object with $L_n/p \gg 1$ behaves like a flexible coil. The dynamics of the conformation of polymers are due to the relatively low energy (typically, few kcal/mol) required to rotate their backbone around C–C single bonds ($k_B T(295 \text{ K}) = 0.593 \text{ kcal/mol}$), while the large L_n/p ratio is due to the mechanisms by which polymers grow: polymerization reactions are chemical processes uniquely capable of producing long, one-dimensional molecules.

Previous work has shown that a crystallizable block located in the core of a block copolymer micelle can lead to its living growth from molecular precursors in solution.^{13,15} This epitaxial addition produces micelles of uniform lengths, yet it does not generate the large L_n/p ratios necessary to observe topological properties comparable to those of polymer molecules. Those results demonstrated an analogy between the crystallization of inorganic and organic crystals in one dimension.

Self-assembly of nanoscale inorganic building blocks (e.g., nanocrystals, nanorods) has been widely studied^{16–20} and traces its roots in earlier and contemporary works on the study of self-assembly in larger colloidal systems,^{21–29} while relying on mechanisms of interaction that are especially relevant at the nanoscale.¹⁸ While a comprehensive discussion of the mechanisms of interaction that drive self-assembly is beyond the scope of this paper, the interested reader is encouraged to peruse recent reviews that summarize exhaustively this complex area of research.^{7,18,20} Self-assembly of colloidal building blocks can proceed in one dimension^{30–35} and with kinetics similar to those of step-growth polymerization.³⁶ These engineered attachment processes are based on controlled aggregation by selective ligand deprotection,³² oriented attachment^{33,37} (driven by electric dipoles or otherwise), or selective binding of regiospecifically functionalized nanocrystals.^{34,38} These approaches typically result in nanocomposites or crystals that possess a relatively limited colloidal stability, aspect ratio, and/or mechanical flexibility. Therefore, while these works and others laid the foundations of static self-assembly of colloidal matter, they cannot assess quantitatively and reliably certain potential similarities between crystallization and polymerization, or between crystals and polymers.

In order to compare quantitatively the growth kinetic and conformation of polymers with the corresponding ones of nanowires, one needs a nanowire “model system” that can be characterized with the same tools—e.g., static light scattering (SLS)—used to characterize polymers. In a previous publication we reported the synthesis of nanowires that are uniquely suited to this challenge: (i) they are covalent crystals of Bi_2S_3 ^{10,39} (i.e., their structure and bonding is representative of inorganic crystals); (ii) they have a near-molecular diameter ($\sim 1.6 \text{ nm}$);^{10,39} (iii) they grow exclusively in length within the growth times we observed and develop little to no branching¹⁰ (i.e., their length is a reliable measure of their growth); (iv) they are colloidally stable¹⁰ (i.e., they can be characterized by light scattering); and (v) their extinction coefficient is known¹⁰ (i.e., the rate of formation of Bi_2S_3 can be quantified).

■ SYNTHESIS OF THE POLYMER-LIKE NANOWIRES

Ultrathin Bi_2S_3 nanowires (cf. Figure 1a–c) were prepared using a previously reported heterogeneous synthesis⁴⁰ whereby a cold oleylamine solution of elemental sulfur is injected into a hot slurry of bismuth(III) citrate in oleylamine¹⁰ (cf. Supporting Information for details). These specific conditions

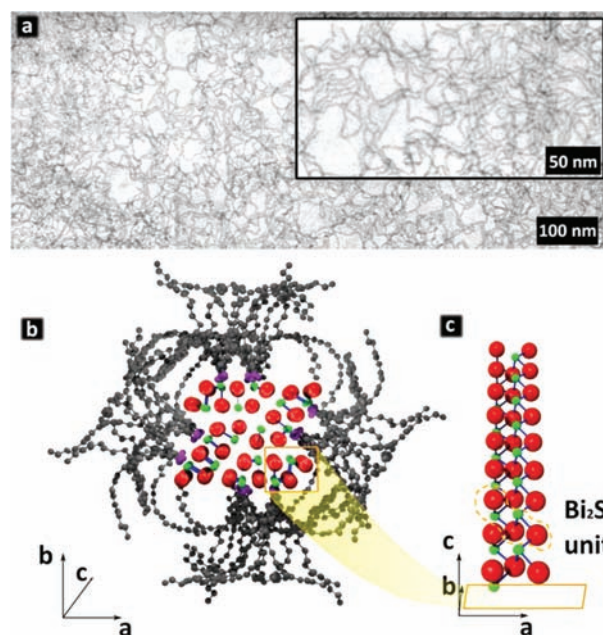


Figure 1. (a) TEM image of Bi_2S_3 nanowires like the ones used in this work; the inset provides a magnified view. (b) Cross-sectional pictorial view of the Bi_2S_3 nanowires, as previously determined³⁹ (green, Bi atoms; red, S atoms; blue, Bi–S covalent bonds; purple, N atoms; gray, C atoms); the inset indicates one of the Bi_2S_3 covalent chains which compose the structure. (c) View of the Bi_2S_3 chains composing the nanowires, along the c -axis of the lattice structure, which highlights the bonding geometry. The orange dashed curve highlights a Bi_2S_3 unit.

yield long, thin, colloidally stable nanowires with a crystalline core of bismuthinite (Bi_2S_3) stabilized by a corona of oleylamine chains (cf. Figure 1).³⁹ Transmission electron microscopy (TEM) reveals that these linear crystals are remarkably uniform in width, with a core thickness of ca. 1.6 nm and lengths of micrometers (cf. Figure 1a).¹⁰ Indeed, they are too long, too thin, and too sensitive to beam damage for their lengths to be determined reliably by electron microscopy (cf. Appendix III in the Supporting Information). Instead, these nanowires are more accurately characterized by light scattering.

■ WORM-LIKE CONFORMATION AND CONTOUR LENGTH OF THE NANOWIRES

The conformation and contour lengths of the growing wires were determined by measuring and modeling the SLS of nanowire suspensions taken at four different reaction times—5, 10, 30, and 120 min after injection—and diluted in toluene. Figure 2a shows the SLS data presented as Holtzer–Casassa^{41,42} plots of $q \cdot P(q)$ versus q , where q is the scattering vector, and $P(q)$ is the form factor of the scattering body. Here, the form factor is expressed as $R_{\theta}/\pi M_0 K c$ (cf. Supporting Information for details), and the solid red lines correspond to the best fits to the data using the form factor for worm-like micelles developed by Sharp and Bloomfield.^{43,44} The qualitative shape of the Holtzer–Casassa curves and the quantitative fits to them show that the nanowires in solution scatter visible light as a worm-like chain would. Similar attempts to reproduce the experimental SLS data using other idealized conformations—i.e., rigid rods and Gaussian coils—were unsuccessful.

As worm-like chains, the nanowires are characterized not only by their contour length L_n but also by a persistence length

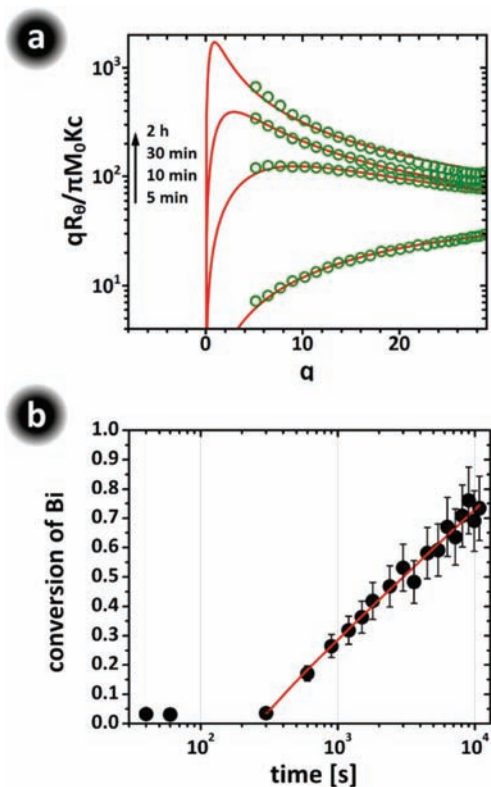


Figure 2. (a) Semilogarithmic plots of $qR_g/\pi M_0 Kc$ vs q from SLS measurements for samples taken at different synthesis times. The lines through the data points represent the best fits with a Zimm–Schulz distribution of lengths. (b) Conversion of Bi into Bi_2S_3 as a function of time (reaction starts at $t = 0$) for the reaction of bismuth citrate with excess sulfur in oleylamine. The linear increase on the semilogarithmic plot denotes a logarithmic increase in the yield with time.

p , which quantifies the persistence of orientational correlations along a set of one-dimensional structures.⁴⁵ Since the diameter of the nanowire is constant throughout growth,¹⁰ we assumed the persistence length to be also constant throughout the reaction and equal to the best-fit value of $p = 17.5$ nm. Remarkably, this persistence length is approximately one-third that of double-stranded DNA.⁴⁶ Under this assumption, the fits of the SLS data indicate that the contour length L_n increased in time—from 180 nm after 5 min, to 200 μm after 2 h—as further confirmed by the increasing ratio of the ordinate of the peak maximum at low q to that of the plateau value at high q (cf. Figure 2a). Table 1 summarizes the values of the other fitting parameters (cf. Supporting Information for details about the fitting procedure).

We confirmed the absence of aggregation (i.e., bundles of nanowires) by determining the mass per unit length of the nanowires, expressed here for convenience as the linear aggregation number N_{aggL} in units of Bi_2S_3 units·nm⁻¹; aggregation would yield N_{aggL} values much larger than those expected for a single wire. We calculated values of $N_{\text{aggL}} = 21$ Bi_2S_3 units·nm⁻¹ for reaction times up to 30 min. N_{aggL} was only slightly larger at 120 min, 29 Bi_2S_3 units·nm⁻¹. These values of N_{aggL} agree remarkably well with our structural model,³⁹ which predicts $N_{\text{aggL}} = 19$ Bi_2S_3 units·nm⁻¹, and are further confirmed by an SLS study of nanowire fragmentation upon sonication (cf. Supporting Information). Table 1 also reports the radius of gyration R_g obtained by treating the

Table 1. Growth Experiments: Fitting Parameters Used To Fit the Experimental Data in Figure 1^a

reaction time [s]	L_n^b [μm]	L_w/L_n^c	N_{aggL} [units·nm ⁻¹]	R_g^d [nm]
300	0.18	1	21	30
600	2	2	21	190
1800	20	2	21	590
7200	200	2	29	1870

^aA single value of persistence length (17.5 nm) was fit from all curves. ^b L_n was obtained by fitting the experimental data using eqs S1 and S3 presented in the Supporting Information. ^c L_w/L_n (the PDI) is obtained from the fitting parameter z , defined as $z = 1/[(L_w/L_n) - 1]$. ^d R_g was evaluated using the formula $R_g^2 = (z + 2)/(z + 1)bL_w/6$, where b is the Kuhn length (in these conditions, $b = 2p$).

nanowires as polydisperse coils with a Zimm–Schulz length distribution.⁴⁷

In summary, light scattering experiments show that the nanowires are individual colloids in solution characterized by a worm-like coiled conformation analogous to that of semiflexible polymer chains, by aspect ratios as large as 10^5 and L_n/p ratios of $\sim 10^4$, and by a persistence length of only 17.5 nm. For the sake of comparison, the longest known synthetic polymers have aspect ratios of $\sim 10^5$ and $L_n/p \approx 10^4$.

■ POLYMER-LIKE GROWTH MECHANISM OF THE NANOWIRES

Following an induction period—typical of nucleation and growth processes, and generally associated with nucleation⁴⁸—the fractional conversion (i.e., reaction yield) of bismuth citrate into Bi_2S_3 increased logarithmically in time (cf. Figure 2b, reaction starts at $t = 0$) up to about 70–80% after 3 h of growth, indicating that the *rate* of conversion decreased in time as $\sim t^{-1}$. The number-average contour length, L_n , of the nanowires (cf. Table 1) increased faster than linearly with time (in fact, the scaling is roughly quadratic in time, $L_n \sim t^2$; see Figure 3a). Furthermore, as shown in Figure 3b, the number concentration of nanowires c (cf. Supporting Information for its derivation) decreased by 2 orders of magnitude during the course of the reaction, as approximated by the scaling relation $c \sim t^{-1}$.

These experimental data suggest that the growth of the nanowires proceeds by two primary mechanisms (cf. Figure 4): an *addition* process whereby “monomer” units add to the ends of existing nanowires in a purely additive manner, or by condensation, and a *coupling* process whereby two nanowires combine end-to-end. These two mechanisms are respectively described by the following rate equations:

$$d\text{Bi}/dt = -2k_{\text{addition}}AN \quad (1)$$

$$dN/dt = -k_{\text{coupling}}N^2 \quad (2)$$

where Bi represents the total amount of *unreacted* bismuth citrate, A is the cross-sectional area of the nanowires, N is the total number of nanowires, and k_{addition} and k_{coupling} are rate constants for the respective processes of “monomer” addition/condensation and nanowire coupling.

Equation 1 describes the first growth mechanism (cf. Figure 1d)—termed “addition”—whereby the “monomer” binds exclusively to the growing tips of the nanowires. The nature of the entity behaving as a monomer is not, within the mechanistic framework described here, essential. Within this framework, any molecular entity (using here the IUPAC

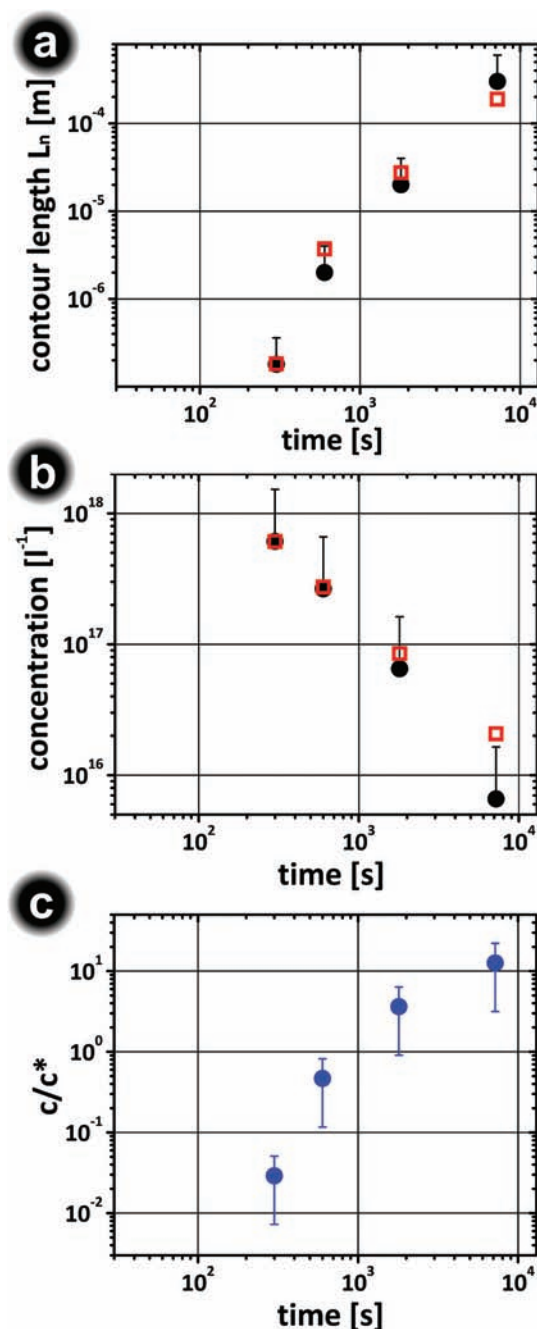


Figure 3. Growth kinetics. (a) Log–log plot of the contour length as a function of time. The black circles represent experimental values obtained by SLS measurements; the red squares correspond to calculated values (eq 4) based on the kinetic model. (b) Log–log plot of the nanowire concentration as a function of the time. As in (a), black circles are experimental values; red squares are model predictions. (c) Log–log plot of the ratio c/c^* between the concentration of the wires and the estimated overlap concentration as a function the time of the reaction. The lines are guides to the eye, and the error bars reflect the known errors in all quantities that were used to extract the experimental value (e.g., extinction coefficient).

definitions of “molecular entity” and “monomer”, which do not exclude that clusters or small nanocrystals be defined as such) that (i) adds to the ends of the nanowires, (ii) increases their length while not changing their chemical nature, and (iii) is not another Bi_2S_3 nanowire can be defined as a monomer. (A similar definition of monomer where “nanowire” is replaced by

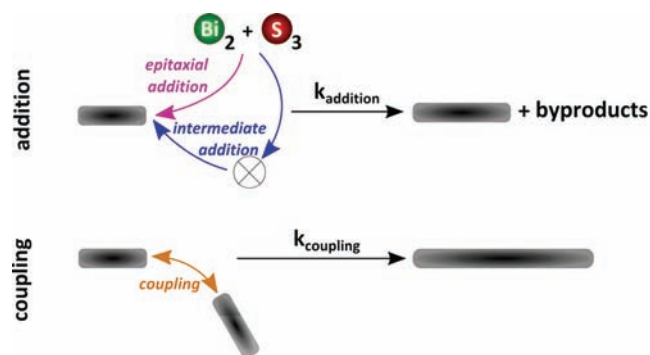


Figure 4. Diagram illustrating the two steps used to describe the growth mechanism of the Bi_2S_3 nanowires. The addition step involves the addition of molecular precursors or intermediates (clusters or complexes) to the tips of the nanowires. This molecular process is expected to produce one or more condensation byproducts. The coupling step involves the attachment of two nanowires by their tips.

“chain” is, not incidentally, applicable to most polymerization processes.) If the monomer were a nanowire there would be no addition process: as it will be shown below, an addition process appears to be necessary to fit the experimental data. The assumption that monomers bind exclusively to the tips is, as mentioned earlier, validated by (i) previously reported microscopy, which showed no change in the diameter of the nanowires, and (ii) optical characterizations of the growing nanowires, which showed no change in the position of the exciton absorption peaks.¹⁰ The origin of this unusual purely one-dimensional growth might lie in the remarkably dense shell of ligands observed on the sides of these nanowires:³⁹ a denser ligand capping should be more effective at opposing a steric hindrance to addition and at reducing the surface energy of the underlying surfaces. The rate constant of the addition/condensation process, k_{addition} , was assumed to be constant in time since the reaction mixture was saturated in the limiting precursor of the reaction (bismuth citrate is present also as a solid in the reaction mixture⁴⁰), while S was in considerable excess ($\text{Bi}:\text{S} = 1:5$). Consequently, we assume that the concentrations of available Bi and S were approximately constant throughout the reaction.

Equation 2 describes the second growth mechanism (cf. Figure 4)—termed “coupling”—whereby nanowires attach end-to-end by a second-order process. To a first approximation, the rate constant k_{coupling} is assumed to be independent of the length of the reacting species, which implies a reaction-limited attachment process. A similar rate equation was proposed by Ribeiro et al. to model the oriented attachment of TiO_2 crystals.^{49,50}

By integrating the rate eqs 1 and 2, we can express the fractional conversion $Y(t)$ of bismuth citrate to Bi_2S_3 as

$$Y(t) - Y_g = \frac{\text{Bi}_g - \text{Bi}}{\text{Bi}_g} = 2 \frac{k_{\text{addition}} A}{k_{\text{coupling}} \text{Bi}_g} \ln(1 + k_{\text{coupling}} N_g (t - t_g)) \quad (3)$$

where the subscript “g” denotes the values of the respective quantities when measured at the onset of growth (i.e., $t = t_g$). Table 2 lists the values of the rate constants and parameters obtained by using eq 3 to fit the data in Figure 2a. The values of Y_g , N_g , and Bi_g obtained in this global fitting analysis are within

Table 2. Fitting Parameters Obtained from the Data in Figure 2a

k_{addition} [$\text{mol}\cdot\text{m}^{-2}\cdot\text{s}^{-1}$]	$(5 \pm 4) \times 10^{-5}$
$k'_{\text{coupling}}{}^a$ [$\text{M}^{-1}\cdot\text{s}^{-1}$]	$(4 \pm 2) \times 10^3$
t_g [s]	300 ± 50
Y_g	0.031 ± 0.026
Bi_g [mmol]	6.13 ± 0.01
N_g [l^{-1}]	$(6 \pm 5) \times 10^{17}$

${}^a k'_{\text{coupling}} \equiv k_{\text{coupling}} V$, where V is the solution volume (here, $V = 38$ mL); in this way, k'_{coupling} is expected to be an intensive quantity of the system, thereby facilitating comparison to other second order attachment processes.

the experimental error of Y , N , and Bi measured on the 5 min sample.

In the absence of significant nanowire branching—an assumption supported by TEM observations—the rate equations can also be used to estimate the average contour length L of the nanowires as a function of time (see Supporting Information for the derivation):

$$L(t) = \left\{ 2 \frac{\nu k_{\text{addition}}}{k_{\text{coupling}} N_g} \ln[1 + k_{\text{coupling}} N_g (t - t_g)] + L_g \right\} [1 + k_{\text{coupling}} N_g (t - t_g)] \quad (4)$$

where ν is the molar volume of Bi_2S_3 . Figure 3a shows good agreement between the contour lengths determined experimentally and those obtained by solving eq 4 with the numerical values listed in Table 2. Alternative models that included all combinations of nucleation, growth, attachment, termination, and fragmentation led consistently to poorer fits to the experimental data—despite having more variables—than our model (cf. Appendix I in the Supporting Information).

SEMIDILUTE GROWTH CONDITIONS

The growth of these nanowires occurred largely under conditions that are defined in polymer science as “semidilute”, whereby the concentration of the nanowires c is higher than the overlap concentration c^* . The model of Ying and Chu⁵¹ for worm-like objects expresses the overlap concentration c^* as

$$c^* = \frac{2^{3/2} M_n}{N_A \left(\frac{b}{2} L_n\right)^{3/2}} \quad (5)$$

Here, M_n is the number-average molecular weight—calculated as $M_n = L_n N_{\text{aggL}} \text{FW}$, where FW is the formula weight of Bi_2S_3 —and N_A is Avogadro’s number. Figure 3c shows a plot of c/c^* as

a function of reaction time. The overlap concentration decreases below the nanowire concentration (i.e., $c/c^* = 1$) approximately 15 min after the initiation of the reaction and coincides with a visually discernible increase in the viscosity of the nanowire suspension. The c/c^* ratio increased steadily as growth continued, indicating that the increase in chain length, which acts to decrease c^* , contributes more strongly than the decrease in nanowire concentration due to coupling.

DISCUSSION

As molecular properties emerge in ligand-capped metal nanocrystals of decreasing dimension,⁵² we hypothesized that the unique properties associated with polymer molecules would also emerge in colloidal nanowires of near-molecular diameter and large aspect ratios. The topological properties of one-dimensional objects derive in large part from the large ratios L_n/p between their contour length and their persistence length. Polymers achieve large (up to $\sim 10^4$) L_n/p ratios by combining the short persistence lengths (~ 1 nm) deriving from the low energetic barrier associated with the rotation of the C–C bonds of their backbone with the large contour lengths (up to $\sim 10^4$ nm) allowed by polymerization.

Our data show that the growth of inorganic crystalline nanowires can resemble many aspects of living polymerization and step-growth polymerization and was primarily responsible for the remarkably large contour lengths and aspect ratios of these nanowires. According to our model, their growth is similar to living polymerization⁵³ in that initiation occurs only at the beginning of the reaction—in the nucleation phase—and the chain ends remain always available—or “active”—to further growth throughout the reaction. (In other words, there is, apparently, no termination.) It is similar to step-growth polymerization in that the addition of monomer to active ends competes with the end-to-end coupling of nanowires. Step growth polymerization can form structures with high aspect ratio because polymer chains can couple together:¹⁴ in the absence of coupling, these nanowires would have grown in 2 h to be $\sim 10 \mu\text{m}$ long instead of $\sim 200 \mu\text{m}$ long. The absence of termination ensured that the wires did not stop growing.

The rates constants of the two growth mechanisms—addition and coupling—can be compared with known rates of polymerization and crystallization (cf. Table 3).

Addition. We can express k_{addition} ($5 \times 10^{-5} \text{ mol}\cdot\text{m}^{-2}\cdot\text{s}^{-1}$) as a turnover frequency, TOF (if we assume, for convenience, that the “monomer” is a Bi_2S_3 unit, then $k_{\text{addition}} \approx 30 \text{ Bi}_2\text{S}_3 \text{ units}\cdot\text{s}^{-1}$), or as a growth rate ($k_{\text{addition}} = 1.6 \text{ nm}\cdot\text{s}^{-1}$). On one hand, the addition process is considerably slower than processes such as catalyzed polymerization (e.g., polyethylene

Table 3. Comparison of the Rates of Addition and Coupling Found for Bi_2S_3 Nanowires and Those Typically Found in Polymerization and Crystallization Processes

	faster processes			colloidal Bi_2S_3 nanowires growth	slower processes	
	catalyzed polymerization	bulk crystallization	diffusion-controlled coupling		step-growth polymerization	colloidal nanocrystal growth
k_{addition} (TOF)	up to 10^3 – 10^4 monomers $\cdot\text{s}^{-1}$ ^a			$\sim 30 \text{ Bi}_2\text{S}_3 \text{ units}\cdot\text{s}^{-1}$	typically 10^3 – 10^2 monomers $\cdot\text{s}^{-1}$ ^c	
k_{addition} (growth rate)	$\sim 10^3 \text{ nm}\cdot\text{s}^{-1}$ ^a	up to $\sim 10^2 \text{ nm}\cdot\text{s}^{-1}$ ^b		$1.6 \text{ nm}\cdot\text{s}^{-1}$	$\sim 10^3 \text{ nm}\cdot\text{s}^{-1}$ ^c	typically 10^4 – $10^2 \text{ nm}\cdot\text{s}^{-1}$
k_{coupling}			$\sim 10^5 \text{ M}^{-1}\cdot\text{s}^{-1}$ ^d	$4 \times 10^3 \text{ M}^{-1}\cdot\text{s}^{-1}$	$\sim 10^3$ – $10^5 \text{ M}^{-1}\cdot\text{s}^{-1}$ ^c	

^aRef 54. ^bRef 55. ^cRef 56. ^dRefs 14, 58, 59, and 63.

can polymerize at a rate of 10^3 – 10^4 insertions per second,⁵⁴ or $\sim 10^3$ nm·s⁻¹) or bulk crystallization (e.g., Si can be grown at rates of 10^2 nm·s⁻¹).⁵⁵ On the other hand, the addition process described here is much faster than that observed in typical step-growth polymerizations ($\sim 10^{-3}$ nm·s⁻¹)⁵⁶ or in nanocrystal growth in organic solvents (typically between 10^{-4} and 10^{-2} nm·s⁻¹).⁵⁷

Coupling. On one hand, the rate of coupling of these nanowires (ca. 4×10^3 M⁻¹·s⁻¹) is much slower than that expected for a process controlled by diffusion (ca. 1×10^5 M⁻¹·s⁻¹).^{14,58,59} On the other hand, the process of coupling is orders of magnitude faster than the coupling observed in step-growth polymerization reactions (typically in the range of $\sim 10^{-3}$ – 10^{-5} M⁻¹·s⁻¹).⁵⁶ Therefore, while we might be intuitively prone to think of the end-to-end coupling of fully formed inorganic crystalline nanowires as an extraordinarily rare event, these results demonstrate that this process can occur at a faster rate than those of common molecular reactions. A nontrivial consequence of this finding is that it suggests that the “reaction-controlled” addition and binding of colloidal nanostructures in solution can be used effectively to mimic molecular reactions within practical time scales.

Light scattering measurements showed that the nanowires adopt a conformation in solution analogous to that of semiflexible polymers: a worm-like conformation characterized by a persistence length ($p = 17.5$ nm) which is approximately 3 times smaller than that of double-stranded DNA. This persistence length implies that these nanowires possess L_n/p ratios of up to $\sim 10^4$, which are larger than those of most polymers. Therefore, while these ultrathin nanowires are still stiffer than most flexible polymers, their worm-like conformation in solution is comparable.

A worm-like conformation can be described as a random flight. In good or theta solvents and in the viscous state, the worm-like conformation of polymer chains at room temperature will typically change over time due to Brownian motion. In 2006, Monkenbusch et al. studied alkyl-substituted polynorbornenes (PNB) in tetrahydrofuran. Interestingly, the authors observed by SLS and SANS that PNB behaves like a flexible coil in good solvent, although neutron spin echo (NSE) experiments showed that the polymer was dynamically frozen.⁶⁰ Therefore, while SLS, SAXS, or SANS experiments can determine that our nanowires display a worm-like conformation, they cannot determine whether the conformation is dynamic or static under the conditions of observation we used (i.e., room temperature, good solvent, and atmospheric pressure). In the case of inorganic nanowires, a contributing or dominant factor to the conformation of the nanowires in solution could also be, for example, defects (e.g., twinning) which could be formed in the atomic structure during its growth.⁶¹ (The nanowires fragment extensively and rapidly under a focused electron beam, preventing us from visualizing twins or other structural defects in their structure by HRTEM.)

The results presented here do not resolve what fraction of the observed persistence length is attributable to dynamic changes in their conformation due to Brownian motion in solution. In other words, we cannot resolve from SLS data whether the persistence length is a result of the flexibility of the nanowires or of a kinked static conformation. Nonetheless, three solid hints—based on extensive electron microscopy (EM) imagery of nanowire samples produced over the course of three years—suggest that the distribution of conformations of the wires is, in fact, due to the thermally activated coiling of

an otherwise linear structure. (i) All EM images show that the nanowires can flex to conform to the flat surface of the TEM grid over length scales that are much larger than the persistence length without breaking. (ii) EM images show that the nanowires are able to form aligned arrays on the EM grid over distances that are again much larger than p . (iii) EM images provide ample evidence of nanowires that are smoothly bent over tens of nanometers or more: kinks due to twinning would lead to stepwise changes in the direction of the nanowires over a few angstroms.⁶¹ A “mechanical” expression of the persistence length of the nanowires as $p \approx Yd^4/k_B T$, where Y is Young’s modulus, d is the diameter of the wire, and $k_B T$ is the thermal energy,¹⁴ yields a Young’s modulus for these nanowires of ~ 10 MPa, which is comparable to that of rubbers, and 3 orders of magnitude smaller than that of bulk Bi₂S₃.⁶² If we assume for a moment that the conformation of the nanowire is indeed due to their mechanical flexibility, this result suggests that the deformation of these wires is not entirely elastic but might be mediated by structural defects.

CONCLUSIONS

This paper reaches three major conclusions: (i) The crystallization of an ensemble of colloidal ultrathin nanowires can occur by mechanisms conceptually identical and quantitatively comparable to those of living step-growth polymerization. (ii) Nanoscale one-dimensional crystals are capable of displaying a topological characteristic of polymers—a worm-like conformation in solution—and possibly more. (iii) Static light scattering can be applied, with appropriate care and corrections, to the study of conformations and growth of colloidal nanowires in solution.

Furthermore, this work establishes a unique experimental model system for the investigation of polymer-like topological properties in inorganic crystals, provides new heuristic guidelines for the synthesis of polymer-like nanowires, and suggests that ultrathin crystals might spontaneously deform under Brownian motion.

ASSOCIATED CONTENT

Supporting Information

Materials and Methods; Appendix I, alternative kinetic models we explored which show that our model produce the best fits of the data; Appendix II, derivation of the kinetic equations used in the manuscript; Appendix III, discussion of the effect of fragmentation on the length of nanowires and how it prevents us from measuring the length of the nanowires with EM; Appendix IV, stochastic growth simulations that offer further confirmation of the proposed kinetic model; Appendix V, evaluation of persistence length from TEM images which yields a value of $p = 14$ nm, remarkably close to the one obtained from SLS (17.5 nm); and Appendix VI, Zimm plots for the SLS data. This material is available free of charge via the Internet at <http://pubs.acs.org>.

AUTHOR INFORMATION

Corresponding Author

mwinnik@chem.utoronto.ca; gozin@chem.utoronto.ca

Present Address

[†]Department of Materials Science & Engineering, Iowa State University of Science and Technology, Ames, IA 50011

Notes

The authors declare no competing financial interest.

■ ACKNOWLEDGMENTS

L.C. thanks the National Science and Engineering Research Council of Canada (NSERC) for a fellowship. K.J.M.B. gratefully acknowledges financial support from the Penn State Center for Nanoscale Science (NSF-MRSEC). M.A.W. thanks NSERC Canada for research support. G.A.O. is Government of Canada Research Chair in Materials Chemistry and Nanochemistry. He is deeply indebted to the Natural Sciences and Engineering Council for strong and sustained support of his research. The authors thank George M. Whitesides, Chad A. Mirkin, and Walther Burchard for valuable comments on the manuscript.

■ REFERENCES

- (1) Cui, Y.; Duan, X. F.; Hu, J. T.; Lieber, C. M. *J. Phys. Chem. B* **2000**, *104*, 5213–5216.
- (2) Huang, M. H.; Mao, S.; Feick, H.; Yan, H. Q.; Wu, Y. Y.; Kind, H.; Weber, E.; Russo, R.; Yang, P. D. *Science* **2001**, *292*, 1897–1899.
- (3) Piraux, L.; George, J. M.; Despres, J. F.; Leroy, C.; Ferain, E.; Legras, R.; Ounadjela, K.; Fert, A. *Appl. Phys. Lett.* **1994**, *65*, 2484–2486.
- (4) Lee, S. H.; Jung, Y.; Agarwal, R. *Nat. Nanotechnol.* **2007**, *2*, 626–630.
- (5) Cheong, S. W.; Mostovoy, M. *Nat. Mater.* **2007**, *6*, 13–20.
- (6) Qin, Y.; Wang, X. D.; Wang, Z. L. *Nature* **2008**, *451*, 809–813.
- (7) Cademartiri, L.; Ozin, G. A. *Concepts of Nanochemistry*; Wiley-VCH: Weinheim, 2009.
- (8) Alivisatos, A. P. *Science* **1996**, *271*, 933–937.
- (9) Cademartiri, L.; Ozin, G. A. *Adv. Mater.* **2009**, *21*, 1013–1020.
- (10) Cademartiri, L.; Malakooti, R.; O'Brien, P. G.; Migliori, A.; Petrov, S.; Kherani, N. P.; Ozin, G. A. *Angew. Chem., Int. Ed.* **2008**, *47*, 3814–3817.
- (11) Wu, Y.; Cui, Y.; Huynh, L.; Barrelet, C. J.; Bell, D. C.; Lieber, C. M. *Nano Lett.* **2004**, *4*, 433–436.
- (12) Liu, C. M.; Yang, S. H. *ACS Nano* **2009**, *3*, 1025–1031.
- (13) Gilroy, J. B.; Gadt, T.; Whittell, G. R.; Chabanne, L.; Mitchels, J. M.; Richardson, R. M.; Winnik, M. A.; Manners, I. *Nat. Chem.* **2010**, *2*, 566–570.
- (14) Rubinstein, M.; Colby, R. H. *Polymer Physics*; Oxford University Press: Oxford, UK, 2003.
- (15) Wang, X. S.; Guerin, G.; Wang, H.; Wang, Y. S.; Manners, I.; Winnik, M. A. *Science* **2007**, *317*, 644–647.
- (16) Pileni, M. P. *J. Phys. Chem. B* **2001**, *105*, 3358–3371.
- (17) Colfen, H.; Antonietti, M. *Angew. Chem., Int. Ed.* **2005**, *44*, 5576–5591.
- (18) Bishop, K. J. M.; Wilmer, C. E.; Soh, S.; Grzybowski, B. A. *Small* **2009**, *5*, 1600–1630.
- (19) Nie, Z.; Petukhova, A.; Kumacheva, E. *Nat. Nanotechnol.* **2010**, *5*, 15–25.
- (20) Gao, Y.; Tang, Z. *Small* **2011**, *7*, 2133–2146.
- (21) Denkov, N. D.; Velev, O. D.; Kralchevsky, P. A.; Ivanov, I. B.; Yoshimura, H.; Nagayama, K. *Langmuir* **1992**, *8*, 3183–3190.
- (22) Denkov, N. D.; Velev, O. D.; Kralchevsky, P. A.; Ivanov, I. B.; Yoshimura, H.; Nagayama, K. *Nature* **1993**, *361*, 26–26.
- (23) Mao, Y.; Cates, M. E.; Lekkerkerker, H. N. W. *Physica A* **1995**, *222*, 10–24.
- (24) Dimitrov, A. S.; Nagayama, K. *Langmuir* **1996**, *12*, 1303–1311.
- (25) van Blaaderen, A.; Ruel, R.; Wiltzius, P. *Nature* **1997**, *385*, 321–324.
- (26) Jiang, P.; Bertone, J. F.; Hwang, K. S.; Colvin, V. L. *Chem. Mater.* **1999**, *11*, 2132–2140.
- (27) Norris, D. J.; Arlinghaus, E. G.; Meng, L. L.; Heiny, R.; Scriven, L. E. *Adv. Mater.* **2004**, *16*, 1393–1399.
- (28) Leunissen, M. E.; Christova, C. G.; Hynninen, A. P.; Royall, C. P.; Campbell, A. L.; Imhof, A.; Dijkstra, M.; van Roij, R.; van Blaaderen, A. *Nature* **2005**, *437*, 235–240.
- (29) Matijevic, E. *Colloid J.* **2007**, *69*, 29–38.
- (30) van der Kooij, F. M.; Kassapidou, K.; Lekkerkerker, H. N. W. *Nature* **2000**, *406*, 868–871.
- (31) Banfield, J. F.; Welch, S. A.; Zhang, H. Z.; Ebert, T. T.; Penn, R. L. *Science* **2000**, *289*, 751–754.
- (32) Tang, Z.; Kotov, N. A.; Giersig, M. *Science* **2002**, *297*, 237–240.
- (33) Cho, K. S.; Talapin, D. V.; Gaschler, W.; Murray, C. B. *J. Am. Chem. Soc.* **2005**, *127*, 7140–7147.
- (34) DeVries, G. A.; Brunnbauer, M.; Hu, Y.; Jackson, A. M.; Long, B.; Neltner, B. T.; Uzun, O.; Wunsch, B. H.; Stellacci, F. *Science* **2007**, *315*, 358–361.
- (35) Yuwono, V. M.; Burrows, N. D.; Soltis, J. A.; Penn, R. L. *J. Am. Chem. Soc.* **2010**, *132*, 2163–2165.
- (36) Liu, K.; Nie, Z. H.; Zhao, N. N.; Li, W.; Rubinstein, M.; Kumacheva, E. *Science* **2010**, *329*, 197–200.
- (37) Yuwono, V. M.; Burrows, N. D.; Soltis, J. A.; Penn, R. L. *J. Am. Chem. Soc.* **2010**, *132*, 2163–+.
- (38) Nie, Z. H.; Fava, D.; Kumacheva, E.; Zou, S.; Walker, G. C.; Rubinstein, M. *Nat. Mater.* **2007**, *6*, 609–614.
- (39) Thomson, J. W.; Cademartiri, L.; MacDonald, M.; Petrov, S.; Calestani, G.; Zhang, P.; Ozin, G. A. *J. Am. Chem. Soc.* **2010**, *132*, 9058–9068.
- (40) Cademartiri, L.; Ozin, G. A. *Philos. Trans. R. Soc. A* **2010**, *368*, 4229–4248.
- (41) Casassa, E. F. *J. Chem. Phys.* **1955**, *23*, 596–597.
- (42) Holtzer, A. *J. Polym. Sci.* **1955**, *17*, 432–434.
- (43) Sharp, P.; Bloomfield, V. A. *Biopolymers* **1968**, *6*, 1201–1211.
- (44) Potschke, D.; Hicld, P.; Ballauff, M.; Astrand, P. O.; Pedersen, J. S. *Macromol. Theory Simul.* **2000**, *9*, 345–353.
- (45) In the case of polymer molecules, p derives typically from the dynamic deformations of the backbone undergoing Brownian motion, with smaller values of p indicating a greater flexibility. This assumption is unwarranted for inorganic crystals which deform by different mechanisms. In this manuscript we do not make use of this assumption.
- (46) Williams, M. C.; Wenner, J. R.; Rouzina, L.; Bloomfield, V. A. *Biophys. J.* **2001**, *80*, 874–881.
- (47) Schmidt, M. *Macromolecules* **1984**, *17*, 553–560.
- (48) LaMer, V. K.; Dinegar, R. H. *J. Am. Chem. Soc.* **1950**, *72*, 4847–4854.
- (49) Ribeiro, C.; Lee, E. J. H.; Longo, E.; Leite, E. R. *ChemPhysChem* **2006**, *7*, 664–670.
- (50) Burrows, N. D.; Yuwono, V. M.; Penn, R. L. *MRS Bull.* **2010**, *35*, 133–137.
- (51) Ying, Q. C.; Chu, B. *Macromolecules* **1987**, *20*, 362–366.
- (52) Jin, R. C. *Nanoscale* **2010**, *2*, 343–362.
- (53) Webster, O. W. *Science* **1991**, *251*, 887–893.
- (54) Gromada, J.; Carpentier, J.-F.; Mortreux, A. *Coord. Chem. Rev.* **2004**, *248*, 397–410.
- (55) Cao, J.; Gao, Y.; Chen, Y.; Zhang, G.; Qiu, M. *Rare Metals* **2011**, *30*, 155–159.
- (56) Flory, P. J. *J. Am. Chem. Soc.* **1939**, *61*, 1518–1521.
- (57) Yang, Y. A.; Wu, H. M.; Williams, K. R.; Cao, Y. C. *Angew. Chem., Int. Ed.* **2005**, *44*, 6712–6715.
- (58) If coupling were diffusion-controlled, it would be described by a Smoluchowski equation of the form $k_{c,diff} = 8\pi R_c(D_i + D_j)$, where $k_{c,diff}$ is the diffusion-controlled coupling rate constant, R_c is the capture radius of the nanowire chain end, and D_i and D_j are the diffusion coefficients of the reacting chains of lengths i and j . For entangled chains, the coupling rate constant would decrease strongly ($D \sim N^{-2}$) with increasing chain length. In Table 3 we estimated a diffusion controlled rate constant by using representative values of viscosity (1000 cP), temperature (373 K), capture radius (0.8 nm), and radius of gyration (500 nm).
- (59) Smoluchowski, M. V. *Phys. Z.* **1916**, *17*, 557–585.
- (60) Monkenbusch, M.; Allgaier, J.; Richter, D.; Stellbrink, J.; Fetters, L. J.; Greiner, A. *Macromolecules* **2006**, *39*, 9473–9479.
- (61) Halder, A.; Ravishankar, N. *Adv. Mater.* **2007**, *19*, 1854–1858.
- (62) Lundegaard, L. F.; Makovicky, E. E.; Boffa-Ballaran, T.; Balic-Zunic, T. *Phys. Chem. Miner.* **2005**, *32*, 578–584.

(63) He, L.; Niemeyer, B. *Biotechnol. Prog.* **2003**, *19*, 544–548.